Structure of a Mouse Immunoglobulin G That Lacks the Entire C_H1 Domain: Protein Sequencing and Small-Angle X-ray Scattering Studies

Takako Igarashi,[‡] Mamoru Sato,[§] Yukiteru Katsube,[§] Koji Takio,[∥] Toshiyuki Tanaka,[‡,⊥] Mamoru Nakanishi,[‡,#] and Yoji Arata*[,‡]

Faculty of Pharmaceutical Sciences, University of Tokyo, Hongo, Tokyo 113, Japan, Institute for Protein Research, Osaka University, Suita, Osaka 565, Japan, and The Institute of Physical and Chemical Research, Wako-shi, Saitama 351, Japan

Received October 3, 1989; Revised Manuscript Received January 9, 1990

ABSTRACT: The structure of a *short-chain* IgG2a antibody, which is a member of the family of mouse anti-dansyl switch variant antibodies with identical variable regions but different heavy-chain constant regions [Dangl, J. L., Parks, D. R., Oi, V. T., & Herzenberg, L. A. (1982) *Cytometry 2*, 395–401], is reported. Amino acid sequencing analyses have demonstrated that in the *short-chain* IgG2a antibody the entire C_H1 domain is deleted whereas the hinge region remains intact. Small-angle X-ray scattering data were collected for the *short-chain* IgG2a antibody and compared with those for the switch variant IgG1, IgG2a, and IgG2b antibodies with the normal heavy chain. It has been concluded that deletion of the C_H1 domain results in a large structural change and the *short-chain* IgG2a antibody possesses an elongated molecular shape with a much smaller hinge angle as compared with the normal IgG2a antibody that is a Y-shaped molecule.

Immunoglobulin G (IgG)[1] consists of two identical heavy chains and two identical light chains. The heavy chains are divided into four domains, V_H, C_H1, C_H2, and C_H3, and the light chain into two domains, V_L and C_L. Dangl et al. (1982) have generated a family of switch variants, producing mouse monoclonal anti-dansyl antibodies with identical V_L, V_H, and C_L in conjunction with different heavy-chain constant regions. A panel of anti-dansyl antibodies reported by Dangl et al. (1982) contains an interesting *short-chain* IgG2a variant, which is unusual in that the apparent molecular weight of its heavy chain is 10K smaller than that of the normal IgG2a heavy chain. It has been shown using domain-specific DNA probes that most of, if not the entire, the C_H1 exon is deleted in this *short-chain* IgG2a antibody (Oi et al., 1984). Oi et al. also reported that this variant antibody has little, if any, segmental flexibility but is able to fix complement as efficiently as the normal IgG2a antibody.

In the present study, we have made protein sequencing analysis of the *short-chain* IgG2a antibody [hereafter designated as IgG2a(s)] and shown that the entire C_H1 domain is actually deleted in IgG2a(s). We will discuss the structure of IgG2a(s) on the basis of the results of small-angle X-ray scattering measurements. A molecular model of the IgG2a(s) antibody will be presented and compared with those for the IgG1, IgG2a, and IgG2b switch variant antibodies with the normal heavy chain.

Materials and Methods

Preparations of Anti-Dansyl Switch Variant Antibodies. Cell lines 27-4.4 (IgG1), 27-13.6 (IgG2a), 27-35.8 (IgG2b), and 27-1B10.7 [IgG2a(s)] have been established as described previously (Dangl et al., 1982). The cells were grown in a Nissui SFM101 serum-free medium. The supernatant was concentrated by using a Millipore Minitan ultrafiltration system and applied to a protein A column (Bio-Rad). Fractions, which were eluted by lowering the pH to 3.0 for the IgG2b antibody and to 4.3 for the IgG1, IgG2a, and IgG2a(s) antibodies, were concentrated, and each of the antibodies was finally made a solution of 50 mM phosphate buffer/150 mM NaCl, pH 7.4, by ultrafiltration.

Sequence Analysis. The IgG2a(s) and IgG2a proteins were reduced and carboxymethylated by using modifications of the procedure by Crestfield et al. (1963); 6 M guanidinium chloride and DTT were used instead of 8 M urea and 2-mercaptoethanol, respectively. The heavy chain was separated from the light chain by using a TSK G3000SWXL HPLC column (TOSOH). The heavy chains of the IgG2a and IgG2a(s) antibodies thus obtained were treated with cyanogen bromide in 70% formic acid as described by Gross (1967). Peptide fragments generated by cyanogen bromide digestion were collected using a TSK G2000SWXL HPLC column (TOSOH) and further purified by reverse-phase HPLC on a Bakerbond WP-butyl column (Baker) with a H_2O/acetonitrile system. A cyanogen bromide fragment obtained from the heavy chain of the IgG2a(s) antibody was subjected to chymotrypsin digestion with an enzyme:substrate ratio of 1:50 for 7 h in 0.1 M NH_4HCO_3, pH 8.0. Digestion products were separated on a Vydac C_4 reverse-phase HPLC column at a flow rate of 0.2 mL/s with a linear gradient of 0–32% acetonitrile in 0.1% trifluoroacetic acid over 16 min. Absorbance was monitored at 207, 275, and 290 nm.

High-performance liquid chromatography was performed on a 1090M HPLC system (Hewlett Packard) equipped with a diode-array detector. Amino-terminal sequence analysis was carried out on an Applied Biosystems 477A protein sequencer equipped with a 120A on-line PTH analyzer.

Antigen Binding. The intensity of emission spectra at 500 nm of ϵ-dansyl-L-lysine was measured in the presence of the antibodies. Excitation wavelength was 335 nm. Concentra-

[‡] University of Tokyo.
[§] Osaka University.
[∥] The Institute of Physical and Chemical Research.
[⊥] Present address: Department of Chemistry, Tohoku University, Aobaku, Sendai 980, Japan.
[#] Present address: Faculty of Pharmaceutical Sciences, Nagoya City University, Mizuhoku, Nagoya 467, Japan.

[1] Abbreviations: DTT, dithiothreitol; HPLC, high-performance liquid chromatography; IgG, immunoglobulin G; IgG2a(s), short-chain mouse monoclonal anti-dansyl IgG2a antibody that lacks the entire C_H1 domain; NMR, nuclear magnetic resonance; PTH, phenylthiohydantoin; SAXS, small-angle X-ray scattering.

0006-2960/90/0429-5727$02.50/0

tions of each of the antibodies were varied with the concentration of the antigen held constant, and the binding constants were determined by Scatchard plots.

Nanosecond Fluorescence Depolarization Measurements. Experiments were performed by using a single photon counting apparatus as described previously (Kinoshita et al., 1981; Kinoshita, 1988). The excitation wavelength was 350 nm, and the emission above 390 nm was collected at 30 °C.

Small-Angle X-ray Scattering (SAXS) Measurements. The X-ray source was a 0.4 × 12 mm spot on the copper anode of a Philips fine-focus X-ray tube operated at 45 kV and 30 mA. The X-ray camera and data acquisition system equipped with a one-dimensional position-sensitive proportional counter have been described previously (Sato et al., 1982; Katagiri et al., 1987). This system can measure SAXS intensities with high accuracy in the scattering angles from 3.0×10^{-3} to 9.0×10^{-2} rad. The temperature of sample solutions, which were introduced into a thin-wall quartz capillary tube, was controlled at 20 ± 0.05 °C by circulating water around the capillary tube. Accumulation times of the scattered intensities were always 3000 s, and 13 measurements were performed successively. Each data set was checked for the effect of aggregation of the sample solution due to X-ray irradiation and also for the possible existence of instrumental artifacts and then accumulated for the improvement of the signal-to-noise ratio of the intensity data.

The scattering intensities recorded on both sides of the primary beam were averaged after subtraction of background intensities. The background intensities were measured by using the buffer solution employed for preparing the sample solutions. The center of the primary beam (zero-angle scattering) was precisely searched so as to attain the best agreement of the scattering intensities at equivalent points on both sides of the zero angles. A slit-smearing effect was corrected by using the algorithm developed by Glatter (1974). The angular variable, h, is defined by $h = 4\pi \sin \theta/\lambda$, where 2θ is the scattering angle and λ the wavelength of X-ray (λ = 1.5418 Å).

The radius of gyration, R_g, and the zero-angle scattering intensity, $I(0)$, were derived from the Guinier plot of SAXS data by a least-squares method (Guinier & Fournet, 1955). The R_g was also estimated from the distance distribution function, $P(r)$ (Glatter, 1982a). The $P(r)$ function, which represents the pair-distance distribution within the same X-ray scatterer, i.e., the intramolecular distance distribution, was calculated by Fourier transformation of the SAXS data (Glatter, 1982a). The maximum particle dimension, D_{max}, was defined as the distance where the $P(r)$ function finally vanishes. The scattering volume, V, which is the hydrate volume of proteins, was estimated from $I(0)$ and Porod's invariant, Q (Porod, 1951; Piltz, 1982), by the equation:

$$V = 2\pi^2 I(0)/Q$$

where

$$Q = \int_0^{\inf} I(h)h^2 \, dh$$

Due to the finite resolution of the scattering parameter data h, the invariant, Q, was numerically integrated from $h = 0$ to $h = h_{max}$, where h_{max} is the largest h value observed. Integration beyond h_{max} was carried out analytically by assuming that $I(h) = ah^{-4}$ for $h > h_{max}$, where a is a constant and determined from $I(h)$ vs h^{-4} plots (Porod, 1951; Piltz, 1982).

In order to assess interparticle interference effects observed in the smaller angle region of the SAXS data, protein solutions with three different concentrations of 2.5, 5.0, and 10 mg/mL were prepared for each of the antibodies. On the basis of the results of careful analyses of the R_g estimated from the Guinier plots, it was concluded that interference effects were negligible at protein concentrations less than 5.0 mg/mL for all of the antibodies.

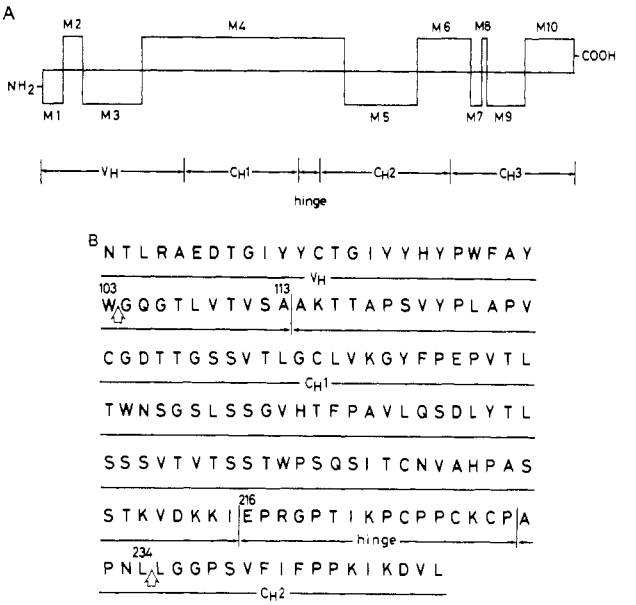

FIGURE 1: (A) Cyanogen bromide fragments M1–M10 of the heavy chain of the IgG2a antibody. (B) Amino acid sequence of fragment M4 given by one-letter code.[3] Possible sites in chymotryptic cleavage of fragment M′, in which the entire C_H1 domain is deleted, are indicated by the open arrows.

Results and Discussion

Amino Acid Sequence of the Heavy Chain of the IgG2a(s) Antibody. As Figure 1 shows, cyanogen bromide cleavage of the heavy chain of the IgG2a antibody, which is of allotype Igh-1a, is expected to give 10 peptide fragments M1–M10.[2] Among these fragments, fragment M4, which consists of 170 amino acid residues and contains the entire C_H1 domain along with the hinge region, is relevant to the present work. Figure 1 also gives the amino acid sequence of fragment M4.[3] Deletion of the entire C_H1 domain would result in a smaller peptide fragment, M4′, with 73 amino acid residues.

In Figure 2, elution profiles on a TSK G2000SWXL HPLC gel filtration column for the products of cyanogen bromide digestion of the heavy chains are compared for the IgG2a and IgG2a(s) antibodies. In the case of the IgG2a(s) antibody, peak 1, which exists in the IgG2a profile, apparently is shifted to become superimposed on peaks 2 and 3, giving peak 1′. No other significant differences are observed for these two antibodies. It was estimated on the basis of the difference in

[2] Sequence data of the V_H region of the switch variant antibodies used in the present study have been given by J. L. Dangl (Ph.D. Thesis, Stanford University, 1986).

[3] The numbering system used in the present paper for the constant region of the heavy chain is based on human myeloma protein Eu (Edelman et al., 1969). The convention of Kabat et al. (1987) has been followed for the numbering of the V_H region of the switch variant antibodies. In numbering the V_H and C_H regions, a number of deletions and insertions are made for achieving the maximum conformity among all the antibodies that have been sequenced so far. In the following discussion, it should therefore be noted that the number of amino acid residues in a given segment does not necessarily coincide with that deduced from the position number of the amino acid residues that bracket the segment. For example, there are 26 residues between Asn-82A, the N terminal residue of M4, and Trp-103; Ala-113, which is the C-terminal residue of the V_H region, is directly followed by Ala-118 that is at the N terminal of the C_H1 region.

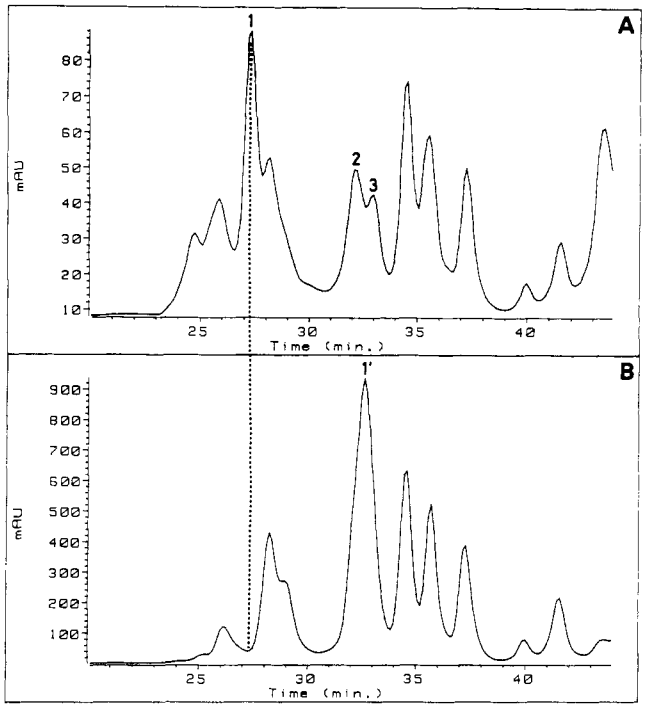

FIGURE 2: Separation of cyanogen bromide fragments obtained from the heavy chain of the IgG2a (A) and IgG2a(s) (B) antibodies on a TSK G3000SWXL HPLC gel filtration column. Eluted at 0.5 mL/s with 10 mM phosphate buffer, pH 6.0, containing 6 M guanidinium chloride. Detection: absorbance at 216 nm.

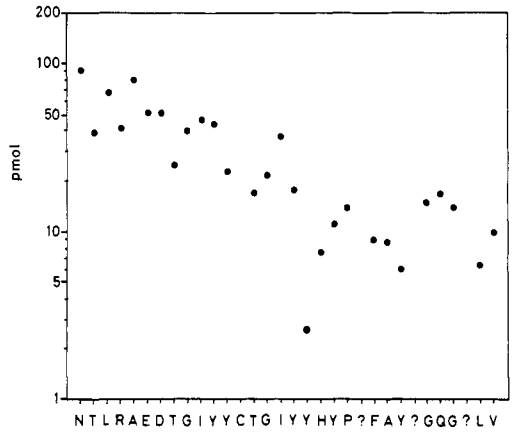

FIGURE 3: Amino acid sequencing of the N-terminal portion of fragment M4′ obtained by cyanogen bromide digestion of the heavy chain of the IgG2a(s) antibody. The logarithms of the yields in picomoles of PTH-amino acid observed on a particular cycle of the automated sequencing are plotted.

retention times that peptide fragments contained in fractions 1 and 1′ are different in molecular weight by approximately 10K. These results strongly suggest that fragments M4 and M4′ are contained in peak 1 and peak 1′, respectively.

The peptide fragment that is characteristic to the IgG2a(s) was separated from other peptide fragments contained in peak 1′ on a Bakerbond reverse-phase WP-butyl HPLC column (data not shown). The IgG2a(s) peptide fragment thus purified was subjected to N-terminal amino acid sequencing analysis, and the result is summarized in Figure 3. This result shows that the N-terminal sequence of this fragment is identical for the first 31 amino acid residues starting at Asn-82A with that of fragment M4 of the native IgG2a antibody[3] (see Figure 1). We therefore conclude that this fragment is M4′.

Fragment M4′ was then subjected to chymotrypsin digestion, and the digestion products were separated on a Vydac C_4 reverse-phase HPLC column. The elution profiles obtained

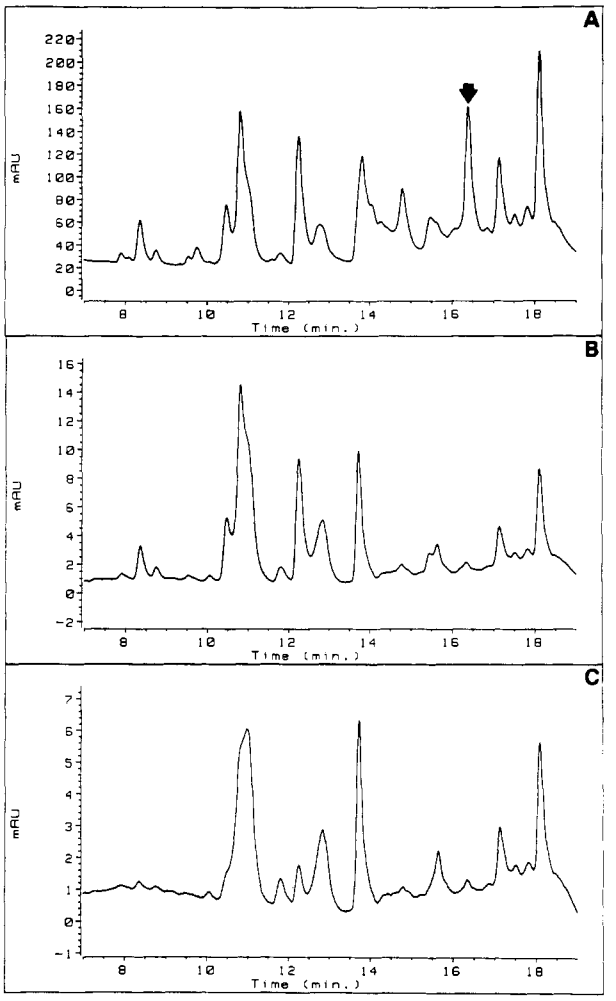

FIGURE 4: Separation of the products of chymotryptic digestion of fragment M4′ on a Vydac C_4 reverse-phase HPLC column. Eluted at 0.2 mL/min with a gradient of 0–32% acetonitrile in 0.1% trifluoroacetic acid over 16 min. Absorbance detected at (A) 207, (B) 275, and (C) 290 nm. The peak indicated by the arrow, which can be detected only at 207 nm, was fractionated and subjected to the protein sequencing analysis.

at 207, 275, and 290 nm are shown in Figure 4. Inspection of Figure 1 indicates that the chymotrypsin cleavage sites, which would bracket the entire C_H1 domain, are Trp-103-Gly-104 and Leu-234-Leu-235.[3] If the entire C_H1 domain is actually deleted in fragment M4′, this chymotryptic peptide would not contain any Trp and Tyr residues. In Figure 4, the major fraction, which is detected at 207 nm but does not show any significant absorption at 275 and 290 nm, is indicated by the arrow. This fraction was collected and subjected to amino acid sequencing analysis, and the result is summarized in Figure 5. Inspection of the relevant part of the sequence of the heavy chain given in Figure 1 indicates that in the chymotryptic fragment the segment $G^{104}QGTLVTVSA^{113}$ is directly connected to the hinge region that starts at Glu-216.[3] The amino acid compositions of the peptides derived by cleavages with cyanogen bromide and chymotrypsin were also analyzed to confirm the above conclusion.

As Figure 2 shows, elution profiles are quite similar to each other except for peaks 1 and 1′, indicating that the C_H1 is the only portion which is different for the IgG2a(s) and IgG2a antibodies. On the basis of the results described above, we conclude that the heavy chain of the anti-dansyl IgG2a(s) antibody lacks the entire C_H1 segment but retains the hinge region intact. Figure 6 schematically summarizes the result obtained in the present work.

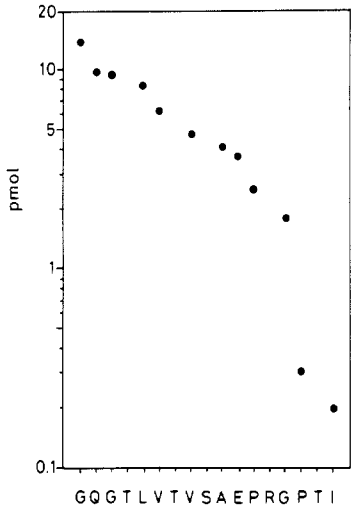

FIGURE 5: Amino acid sequencing of a chymotryptic fragment shown in Figure 4 by the arrow. Plotted as in Figure 3.

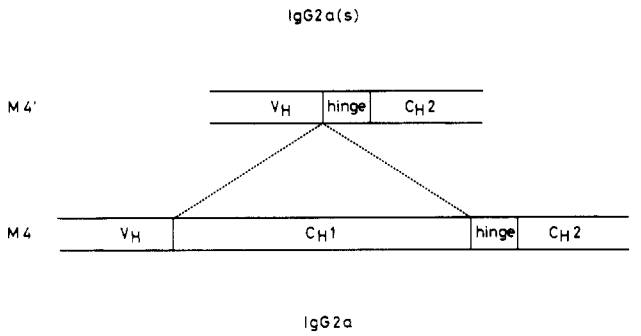

FIGURE 6: Schematic drawing of fragments M4 and M4'.

Adetugbo et al. (1977) have reported a variant of a mouse myeloma IgG1 protein that lacks the entire C_H1 exon and possesses the V_H domain directly connected to the hinge. The IgG2a(s) antibody, which is another example of a mouse antibody with the same type of deletion, is a member of the switch variant antibodies with the known specificity and can therefore make it possible to discuss, for example, the effect of the deletion of the C_H1 domain on the global solution structure of the antibody molecule and also on the structure of the antigen binding site.

Small-Angle X-ray Scattering Measurements. The IgG2a(s) antibody was examined by small-angle X-ray scattering, and the result was compared with those obtained by using other members of the switch variant antibodies. The molecular parameters, R_g, D_{max}, and V, obtained for each of the IgG molecules are summarized in Table I. All of the molecular parameters for IgG2a(s) are in good agreement within experimental error with those for the rest of the switch variant IgG molecules. However, as Figure 7 shows, the $P(r)$ functions calculated from the experimental SAXS data showed significantly different profiles for the series of the switch variant antibodies, IgG1, IgG2a, IgG2a(s), and IgG2b. The $P(r)$ function obtained for IgG2a(s) is symmetrical. By contrast, the $P(r)$ functions for IgG1, IgG2a, and IgG2b are asymmetrical with more than two maxima. These three antibodies possess in common the first maximum around $r = 40$ Å, whereas the second maximum appears at $r = 70$ Å for the IgG1 and at $r = 80$ Å for the IgG2a and IgG2b antibodies. In addition, the relative heights of the first and second maxima are quite different for the three antibodies. These results strongly suggest that the shape of IgG2a(s) in solution is significantly different from the other members of the switch variant antibodies.

Table I: Molecular Parameters Derived from the SAXS Data for Mouse Anti-Dansyl IgG1, IgG2a, IgG2a(s), and IgG2b Switch Variant Antibodies[a]

	R_g[b] (Å)	R_g[c] (Å)	D_{max} (Å)	V ($\times 10^5$ Å^3)
IgG1	49.6 (4)	50.7 (3)	160	2.6
IgG2a	50.5 (3)	51.7 (3)	160	2.7
IgG2a(s)	50.9 (4)	51.7 (4)	165	2.6
IgG2b	51.4 (4)	53.9 (3)	170	2.6

[a] The values given in parentheses are the standard deviations obtained by a least-squares procedure. [b] R_g derived from the Guinier plots. [c] R_g derived from the $P(r)$ functions.

In order to obtain structural information for each of the antibodies, we simulated the molecular model for each of the antibodies on the basis of the $P(r)$ functions. SAXS simulation analyses reported so far for IgG were performed in the reciprocal space using $I(h)$ data [see Piltz et al. (1970, 1977) and references cited therein]. In the present analyses, simulation was performed in the real space by using the $P(r)$ functions, because the calculation in the reciprocal space using $I(h)$ data tends to be ambiguous in fitting simulated $I(h)$ profiles with those determined experimentally in the smaller angle region around the primary beam (Glatter, 1982b).

The three-dimensional structure of proteins cannot uniquely be determined solely on the basis of the SAXS data. This is because spatial averaging of protein molecules in solution with respect to the X-ray beam and the resultant one-dimensional intensity data reduce the number of molecular parameters available. Therefore, prior to the simulation analyses, one has to provide the initial model on the basis of structural information such as that of electron microphotographs. In their SAXS study of the structure of a human IgG molecule in solution, Piltz et al. (1970) made use of electron microscopic (Valentine & Green, 1967) and hydrodynamic (Noelken et al., 1965) data. In the present SAXS study, X-ray crystallographic data for a human IgG antibody Kol and its Fab and Fc fragments (Deisenhofer et al., 1976; Huber et al., 1976; Matsushima et al., 1978; Marquart et al., 1980; Deisenhofer, 1981) were used for the construction of the initial models.

We started from two kinds of initial models, i.e., one for IgG2a(s), which lacks the entire C_H1 domain, and the other for the rest of the switch variant antibodies. In these models, the shapes of the Fab and Fc regions were approximated by the assembly of spheres with the identical radius. In view of the highest resolution of the SAXS data (h_{max}), the radius of the spheres was chosen to be 8.5 Å. With the use of these models, the $P(r)$ functions were simulated with different hinge angles ranging from 0° to 180° and also with different combinations of the number and arrangement of the spheres in the Fab and Fc regions. In the process of simulation for the number and arrangement of the spheres, the R_g and D_{max} data obtained for each of the intact antibodies were taken into account. It was found that the shape of the simulated $P(r)$ function is extremely sensitive to the hinge angle employed. By contrast, the result of simulation is much less sensitive to the number and arrangement of the spheres for the Fab and Fc regions. Finally, the models given in Figure 8 were employed to achieve a best fit between experimental and simulated $P(r)$ functions. In these models, the number of spheres is 68 and 76 for the IgG2a(s) and the rest of the antibodies, respectively. At this final stage of simulation, we used the hinge angle as the only adjustable parameter. As Figure 7 shows, the profiles of the experimental $P(r)$ functions characteristic for the IgG1, IgG2a, and IgG2b antibodies have successfully been reconstructed by the simulation. Three maxima, which are observed in the calculated $P(r)$ function

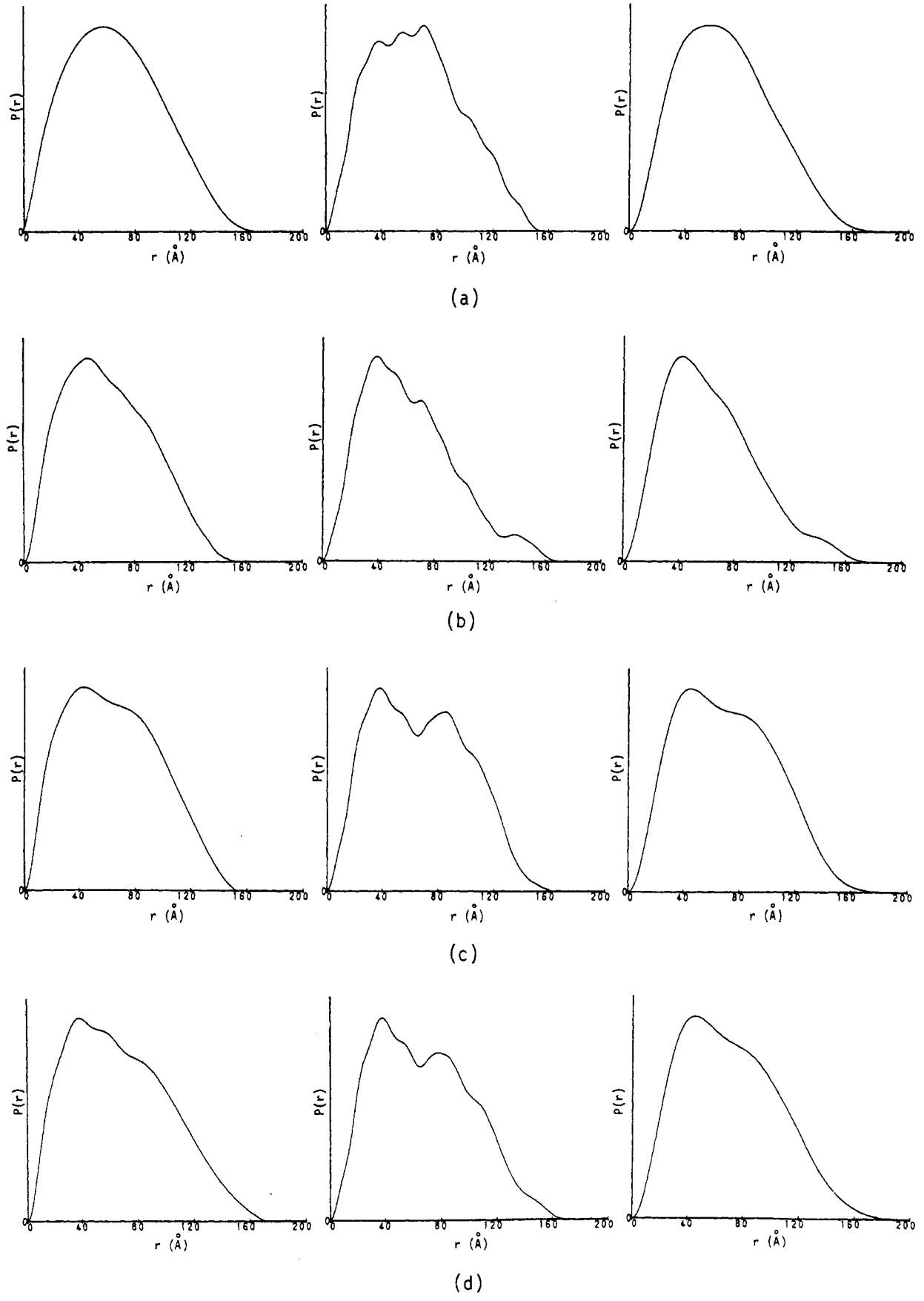

FIGURE 7: Distance distribution functions, $P(r)$, for (a) IgG2a(s), (b) IgG1, (c) IgG2a, and (d) IgG2b. The $P(r)$ functions calculated from the experimental SAXS data are given on the left of each of the panels. The $P(r)$ values obtained by using optimum hinge angles with and without the temperature factor into consideration are reproduced on the right and in the middle of the panels, respectively. The mean deviations from the equilibrium position, σ, employed for the calculation were (a) 7.6, (b) 5.0, (c) 8.7, and (d) 8.7 Å.

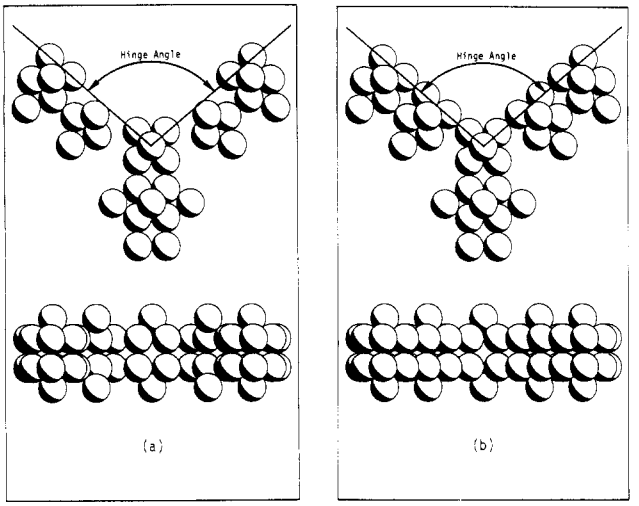

FIGURE 8: Initial models used for the simulation of the SAXS data for (a) IgG2a(s) and (b) IgG1, IgG2a, and IgG2b. The number of spheres is (a) 68 and (b) 76. The radius of each of the spheres is 8.5 Å. Side and top views are given for each of the models.

for the IgG2a(s) antibody (in the middle panel of Figure 7a), are not the ripples due to the coarse grain of the model antibodies, but can provide information about the hinge angle. With the increase of the hinge angle, the first and third maxima become dominant and the second maximum around $r = 50$ Å disappears. In addition, the relative height of the first maximum and the position of the third maximum are highly dependent on the hinge angle (data not shown).

The agreement between the experimental and simulated $P(r)$ functions is not quite satisfactory in the distance region around $r = 70$ Å. This is especially true in the cases of the IgG2a and IgG2b antibodies. It is quite possible that the unsatisfactory agreement between the experimental and calculated $P(r)$ data has resulted from the effect of thermal vibration of the antibody molecules. We therefore introduced a thermal vibrational parameter, B, to the simulation analyses. By taking into account the isotropic mean square deviation from the equilibrium position (Blundel & Johnson, 1976), the temperature factor was introduced to define $I(h)_T$ as

$$I(h)_T = I(h) \exp(-Bh^2/8\pi^2)$$

where B is given by using σ, which is the mean deviation from the equilibrium position:

$$B = 8\sigma^2\pi^2$$

From the convolution theorem of Fourier transformation, $P(r)$ functions were calculated by using the $I(h)_T$. The $P(r)_T$ values thus obtained are given in Figure 7. Obviously, agreements between the experimental and simulated $P(r)$ data have been greatly improved. The molecular models thus obtained on the basis of the simulation analyses are presented in Figure 9. These results indicate that the hinge angle is greatly reduced when the C_H1 domain is deleted, rendering the IgG2a(s) antibody elongated in shape. It was also shown that the IgG2a and IgG2b antibodies take a Y shape as widely accepted for the antibody molecule. It is of interest that the IgG1 antibody is of a T shape.

The switch variant antibodies were also examined by the nanosecond fluorescence depolarization technique. Time dependence of the emission anisotropy of ε-dansyl-L-lysine in the combining site of each of the antibodies was examined, and the results are given in Figure 10. The results obtained for the IgG1, IgG2a, and IgG2b antibodies are consistent with those reported previously by Oi et al. (1983). In view of the

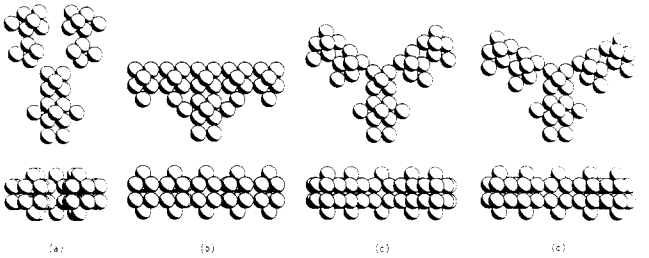

FIGURE 9: Molecular models obtained for (a) IgG2a(s), (b) IgG1, (c) IgG2a, and (d) IgG2b. Hinge angles for each of these models are (a) 15°, (b) 180°, (c) 100°, and (d) 120°. Side and top views are given for each of the models.

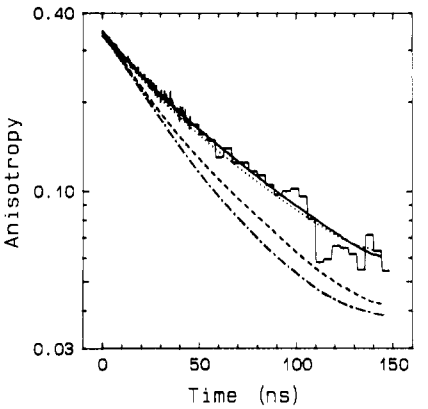

FIGURE 10: Time dependence of the emission anisotropy at 30 °C of ε-dansyllysine in the combining site of each of the switch variant antibodies. For the IgG2a(s) antibody, both experimental data and nonlinear least-squares best fit of the observed data are given by solid lines. Results obtained for IgG1 (···), IgG2a (- - -), and IgG2b (-·-) antibodies are also presented. Experimental details are given under Materials and Methods.

SAXS results described above, we suggest that the fluorescence polarization data have to be interpreted with care by taking into account the shape of each of the antibodies. The IgG2a and IgG2b data may primarily be interpreted as representing the flexibility of the hinge region in each of these antibodies. The fluorescence polarization decay observed for the IgG2a(s) antibody are much slower than those for the IgG2a antibody and become quite similar to those for the IgG1 antibody. It should be noted that the IgG2a(s) antibody retains the hinge region intact and, in addition, is lower in molecular weight by 24K due to the lack of the C_H1 domain as compared to antibodies with the normal heavy chain. It appears that the hinge region can no longer contribute to the segmental flexibility in the absence of the C_H1 domain. Presumably, the elongated shape of the IgG2a(a) molecule with the small hinge angle is reponsible for the reduced segmental flexibility. It may also be necessary to take into account the role of the shape of the molecule in interpreting the fluorescence polarization decay data observed for the IgG1 antibody. How the deletion of the C_H1 domain affects the mode of domain–domain interactions, leading to a large change in the shape of the IgG2a(s) antibody molecule, remains to be clarified.

The binding constants determined for the IgG1, IgG2a, and IgG2b antibodies are quite consistent with those reported by Dangl et al. (1982). The IgG2a(s) antibody is virtually identical in binding constant with the rest of the switch variant antibodies. This indicates that deletion of the C_H1 domain does not affect the affinity of antigen binding.

In conclusion, (1) the IgG2a(s) antibody lacks the entire C_H1 but retains its hinge region intact, and (2) it possesses a much smaller hinge angle as compared with the normal IgG2a antibody, but (3) the C_H1 deletion does not affect the

affinity of antigen binding. It is of great interest to know how and to what extent the effect of deletion of one of immunoglobulin domains is transmitted to other domains. The IgG2a and IgG2a(s) antibodies would provide us with an ideal system for the elucidation of these problems. We have recently reported that stable isotope aided NMR can be effective in obtaining information about the structure of the main chains of antibody molecules (Kato et al., 1989a,b). Structural analyses of the IgG2a and IgG2a(s) antibodies specifically labeled by ^{13}C at the carbonyl carbons of methionine and tryptophan residues are underway.

ACKNOWLEDGMENTS

We are grateful to Professor L. A. Herzenberg, Stanford University, and Dr. V. T. Oi, Becton Dickinson Immunocytometry Systems, for generously providing us with the switch variant cell lines used in the present experiment. We also thank Dr. K. Kinoshita, Keio University, for the nanosecond fluorescence depolarization measurements of the switch variant antibodies and also for his helpful discussion. Thanks are due to Professor K. Titani, Fujita-Gakuen Health University, for his helpful comments on the protein sequencing of the IgG2a(s) antibody.

REFERENCES

Adetugbo, K., Milstein, C., & Secher, D. S. (1977) *Nature 265*, 299–304.

Blundel, T. L., & Johnson, L. N. (1976) *Protein Crystallography*, pp 121–122, Academic Press, London.

Crestfield, A. M., Moore, S., & Stein, W. H. (1963) *J. Biol. Chem. 238*, 622–627.

Dangl, J. L., Parks, D. R., Oi, V. T., & Herzenberg, L. A. (1982) *Cytometry 2*, 395–401.

Deisenhofer, J. (1981) *Biochemistry 20*, 2365–2370.

Deisenhofer, J., Colman, P. M., Epp, O., & Huber, R. (1976) *Hoppe-Seyler's Z. Physiol. Chem. 357*, 1421–1434.

Edelman, G. M., Cunningham, B. A., Gall, W. E., Gottlieb, P. D., Rutishauser, U., & Waxdal, M. J. (1969) *Proc. Natl. Acad. Sci. U.S.A. 63*, 78–85.

Glatter, O. (1974) *J. Appl. Crystallogr. 7*, 147–153.

Glatter, O. (1982a) in *Small Angle X-ray Scattering* (Glatter, O., & Kratky, O., Eds.) pp 130–138, Academic Press, New York.

Glatter, O. (1982b) in *Small Angle X-ray Scattering* (Glatter, O., & Kratky, O., Eds.) pp 329–359, Academic Press, New York.

Gross, E. (1967) *Methods Enzymol. 11*, 238–255.

Guinier, A., & Fournet, G. (1955) *Small-Angle Scattering of X-Rays*, p 126, Wiley, New York.

Huber, R., Deisenhofer, J., Colman, P. M., & Matsushima, M. (1976) *Nature 264*, 415–420.

Kabat, E. A., Wu, T. T., Reid-Miller, M., Perry, H. M., & Gottesman, K. S. (1987) *Sequences of Proteins of Immunological Interest*, 4th ed., U.S. Department of Health and Human Services, National Institutes of Health, Washington, DC.

Kakagiri, C., Sato, M., & Tanaka, N. (1987) *J. Biol. Chem. 262*, 15857–15861.

Kato, K., Matsunaga, C., Nishimura, Y., Waelchli, M., Kainosho, M., & Arata, Y. (1989a) *J. Biochem. 105*, 867–869.

Kato, K., Nishimura, Y., Waelchli, M., & Arata, Y. (1989b) *J. Biochem. 106*, 361–364.

Kinoshita, K. (1988) *Subcell. Biochem. 13*, 55–88.

Kinoshita, K., Jr., Kataoka, R., Kimura, Y., Gotoh, O., & Ikegami, A. (1981) *Biochemistry 20*, 4270–4277.

Marquart, M., Deisenhofer, J., & Huber, R. (1980) *J. Mol. Biol. 141*, 369–391.

Matsushima, M., Marquart, M., Jones, T. A., Colman, P. M., Bartels, K., Huber, R., & Palm, W. (1978) *J. Mol. Biol. 121*, 441–459.

Noelken, M. E., Nelson, C. A., Buckley, C. E., III, & Tanford, C. (1965) *J. Biol. Chem. 240*, 218–224.

Oi, V. T., Vuong, T. M., Hardy, R. R., Reidler, J., Dangl, J., Herzenberg, L. A., & Stryer, L. (1983) *Nature 307*, 136–140.

Oi, V. T., Hsu, C., Hardy, R., & Herzenberg, L. A. (1984) in *Cell Fusion: Gene Transfer and Transformation* (Beers, R. F., Jr., & Bassett, E. G., Eds.) pp 281–287, Raven Press, New York.

Piltz, I. (1982) in *Small Angle X-ray Scattering* (Glatter, O., & Kratky, O., Eds.) pp 250–251, Academic Press, New York.

Piltz, I., Puchwein, G., Kratky, O., Herbst, M. M., Haager, O., Gall, W. E., & Edelman, G. M. (1970) *Biochemistry 9*, 211–219.

Piltz, I., Schwarz, E., & Palm, W. (1977) *Eur. J. Biochem. 75*, 195–199.

Porod, G. (1951) *Kolloid-Z. 124*, 83–114.

Sato, M., Kato, M., Kasai, N., Hata, Y., Tanaka, N., Kakudo, M., Tanaka, M., & Ozawa, T. (1982) *Biochem. Int. 5*, 595–602.

Valentine, R. C., & Green, N. M. (1967) *J. Mol. Biol. 27*, 615–617.